Identification of Novel Syncytiotrophoblast Membrane Extracellular Vesicles Derived Protein Biomarkers in Early-onset Preeclampsia: A Cross-Sectional Study.

Toluwalase Awoyemi DPhil[1*], Shuhan Jiang MB;BS[1], Bríet Bjarkadóttir DPhil[1], Ms. Maryam Rahbar MSc[1], Prasanna Logenthiran MB;BS[1], Gavin Collett PhD[1], Wei Zhang PhD[1], Adam Cribbs PhD[2], Ana Sofia Cerdeira PhD[1] & Manu Vatish DPhil[1]

1 Nuffield Department of Women's & Reproductive Health, University of Oxford, Oxford, United Kingdom

2 Nuffield Department of Orthopaedics, Rheumatology and Musculoskeletal Sciences, University of Oxford, Oxford, United Kingdom

***Corresponding author:** Dr Manu Vatish, MBBCh, BA (Hons), DPhil, MA, FMRCOG

Manu.vatish@wrh.ox.ac.uk, Phone number- +441865221009, Fax number-01865769141

Address: Nuffield Department of Women's and Reproductive Health, University of Oxford, Women's Centre, John Radcliffe Hospital, Oxford OX3 9DU, United Kingdom

Abstract

Background: Preeclampsia (PE), a multi-systemic hypertensive pregnancy disease that affects 2-8% of pregnancies worldwide, is a leading cause of adverse maternal and fetal outcomes. Current clinical PE tests have a low positive predictive value for PE prediction and diagnosis. The placenta notably releases extracellular vesicles from the syncytiotrophoblast (STB-EV) into the maternal circulation.

Objective: To identify a difference in placenta and STB-EV proteome between PE and normal pregnancy (NP), which could lead to identifying potential biomarkers and mechanistic insights.

Methods: Using ex-vivo dual lobe perfusion, we performed mass spectrometry on placental tissue, medium/large and small STB-EVs isolated from PE (n = 6) and NP (n = 6) placentae. Bioinformatically, mass spectrometry was used to identify differentially carried proteins. Western blot was used to validate the identified biomarkers. We finished our investigation with an in-silico prediction of STB-EV mechanistic pathways.

Results: We identified a difference in the STB-EVs proteome between PE and NP. Filamin B, collagen 17A1, pappalysin-A2, and scavenger Receptor Class B Type 1) were discovered and verified to have different abundances in PE compared to NP. In silico mechanistic prediction revealed novel mechanistic processes (such as abnormal protein metabolism) that may contribute to the clinical and pathological manifestations of PE.

Conclusions: We identified potentially mechanistic pathways and identified differentially carried proteins that may be important in the pathophysiology of PE and are worth investigating because they could be used in future studies of disease mechanisms and as biomarkers.

Funding: This research was funded by the Medical Research Council (MRC Programme Grant (MR/J0033601) and the Medical & Life Sciences translational fund (BRR00142 HE01.01)

Keywords: Syncytiotrophoblast membrane extracellular vesicles (STB-EVs), Preeclampsia, Biomarkers, Proteomics, Placenta EVs, mechanisms

Introduction

Preeclampsia (PE) is a significant cause of maternal and neonatal morbidity and mortality, affecting 2-8% of all pregnancies(Lisonkova & Joseph, 2013). It is characterized by hypertension (systolic blood pressure ≥ 140mmHg / diastolic pressure ≥ 90mmHg), and either proteinuria (protein/creatinine ratio of ≥ 30 mg/mmol or more), or evidence of maternal acute kidney injury, liver dysfunction, neurological abnormalities, hemolysis, or thrombocytopenia, and/or fetal growth restriction.("ACOG Practice Bulletin No. 202: Gestational Hypertension and Preeclampsia," 2019; Brown et al., 2018) Predicting or early detection of PE is thus of extreme importance to reduce the chance of long term complications but this has been challenging due to the limitations of current predictive models and biochemical tests (which lack in positive predictive value)(Zeisler et al., 2016). The existing tests perform far better in ruling out rather than ruling in PE. They are also most effective shortly before the onset of the disease and within a specific time frame (1 or 2 weeks) rather than earlier in pregnancy(Thadhani et al., 2022).

The pathophysiology of PE implicates the placenta. It is known that PE can occur in trophoblastic tumors (without the presence of a fetus); that PE is more common in multiple pregnancy (with greater placental mass) and that it has occurred in ectopic pregnancies (excluding the involvement of the uterus)(Billieux et al., 2004; Hailu et al., 2017; C. W. G. Redman et al., 2022; Soto-Wright et al., 1995). Finally, delivery of the placenta (irrespective of gestational age) is currently the only cure for the condition(C. Redman, 2014).

The placental syncytiotrophoblast (STB) layer, the interface between the fetus and the mother which lies in direct contact with the maternal circulation. EVs, including STB-EVs, are membrane-bound and cell-derived particles that carry different cargos, including proteins, ribonucleic acid (RNA), deoxyribonucleic acid (DNA) and lipids(Raposo & Stoorvogel, 2013). EVs are based on size into medium/large STB-EVs (MVs, 201–1000nm) or small STB-EVs

(≤200nm)(Dragovic et al., 2015a). The release of syncytiotrophoblast extracellular vesicles (STB-EVs), including both size ranges, into the maternal circulation increases with gestation and is further elevated in PE (Germain et al., 2007; Goswamia et al., 2006).Variations in cargo content are evident among different subsets of syncytiotrophoblast-derived extracellular vesicles (STB-EVs), with medium/large STB-EVs (m/lSTB-EVs) showing higher levels of total RNA and total protein in comparison to small STB-EVs (sSTB-EVs)(Zabel et al., 2021). Additionally, distinct miRNA profiles have been noted to differ in abundance between these subsets. While limited studies have investigated disparities in EV subtypes, Keerthikumar et al reported that exosomes and other small extracellular vesicles (EVs) have a more pronounced impact on cell migration and proliferation than the larger EVs known as ectosomes (Keerthikumar et al., 2015) . Furthermore, Minciacchi et al demonstrated that large EVs exhibit greater efficiency in reprogramming fibroblasts and promoting the formation of endothelial cell tubes when compared to small EVs(Minciacchi et al., 2017).

In addition, when it comes to immune cell-derived EVs, large EVs were found to induce the secretion of Th2-associated cytokines, while both medium and small EVs (pelleted at 10,000g and 100,000g) triggered the release of Th1 cytokines(Tkach et al., 2017).These functional distinctions were also observed in STB-EVs. Specifically, our investigation unveiled that normal pregnancy (NP) medium/large-sized STB-EVs significantly enhanced the transcriptional expression of pro-inflammatory cytokines in contrast to pathological (PE) medium/large-sized STB-EVs(Awoyemi et al., 2021). However, there was no significant difference in the small STB-EV population between the two groups, although, in general, NP small STB-EVs exhibited a slight upregulation of the same cytokines(Awoyemi et al., 2021). It is reasonable to conduct further in-depth exploration into the qualitative functional properties of distinct STB-EVs, with the initial step being a comprehensive characterization of these

diverse subtypes. The presence of proteins, RNA species and DNA in EVs combined with their constitutional release as inter-cellular signaling moieties means they also have potential in disease prediction and diagnosis. Notably, these distinct STB-EV subtypes have also been identified in the bloodstream. Nakahara et al extensive review compiles a collection of studies that have specifically isolated various subtypes of EVs from maternal plasma(Nakahara et al., 2020). In this study, we performed proteomic analysis of placenta and STB-EVs in PE and NP to identify potential placenta-derived biomarkers. We also conducted in silico analysis on the proteomes to detect potential molecular targets, mechanisms, and processes of PE.

Methods

Ethics approval and patient information

Oxfordshire Research Ethics Committee C (07/H0606/148) approved this study. Normal pregnancy was a healthy singleton pregnancy with normal maternal blood pressure. PE was defined as new (after 20 weeks) systolic blood pressure 140 mmHg or diastolic pressure 90 mmHg, proteinuria (protein/creatinine ratio of 30 mg/mmol or more). None of our patients had maternal acute kidney injury, liver dysfunction, neurological features, haemolysis, thrombocytopenia, and/or foetal growth restriction. This study included only early-onset PE patients (diagnosed before 34 weeks gestation). After informed consent, placenta was obtained from women undergoing elective caesarian section without labor were collected.

Placenta sample preparation and syncytiotrophoblast membrane extracellular vesicles (STB-EVs) enrichment.

Placenta biopsies were obtained adjacent to the perfused lobe and immediately frozen at -80^{o}C pending transfer to the Target Discovery Institute (Oxford) for proteomic analysis. We obtained STB-EVs via placental perfusion as previously described(Dragovic et al., 2015b). Our

STB-EV enrichment and categorization process has been deposited on EV Track ([http://www.EVTRACK.org], **EV-TRACK ID: EV 220157**) with a score of 78% (the average score on EV track for 2021 is 52 %). Full details can be found in the supplemental data.

Characterization of syncytiotrophoblast membrane extracellular vesicles (STB-EVs)

Enriched STB-EVs were resuspended in filtered phosphate buffered saline (fPBS) and characterized with bicinchoninic acid (BCA) assay (for protein concentration) and nanoparticle tracking analysis (NTA) (for particle number and size profile). We also phenotyped the STB-EVs with transmission electron microscopy (for morphology), flow cytometry (BD Biosciences, LSRII), and western blot (for immunophenotyping). Flow cytometric analysis was performed using antibodies to placental alkaline phosphatase – PLAP- (to confirm syncytiotrophoblast origin), CD 41 (to identify co-isolated platelet EVs, CD235 a/b (to identify co-isolated red blood cell EVs), HLA class I and II (to identify co-isolated white blood cell EVs). Western blot was probed for placental alkaline phosphatase (PLAP [1.667 mg/ml] at 1:1000 dilution in house antibody), the known EV markers CD 63 ([200ug/ml] at 1:1000 dilution, Sc-59286, Santa Cruz Biotechnology), ALIX ([200ug/ml] at 1:1000 dilution, Sc-53538, Santa Cruz Biotechnology) and the known negative EV marker Cytochrome C ([200ug/ml] at 1:1000 dilution, Sc-13156, Santa Cruz Biotechnology) as recommended by the international society for extracellular vesicles (ISEV) and subsequently incubated with the corresponding secondary antibody anti-mouse, or anti-rabbit polyclonal goat immunoglobulins/HRP (at 1: 2000 dilution, Dako UK Ltd, Cambridgeshire UK). Details of nanoparticle tracking analysis and transmission electron microscopy can be found in the supplemental data.

Sample preparation for Mass Spectrometric analysis and bioinformatic analysis of proteomic data from placenta tissue, medium/large, and small STB-EVs

STB-EVs and placental tissue samples were processed for liquid chromatography mass spectrometry (LC-MS) (Target Discovery Institute, Oxford). Briefly, STB-EVs and placental tissue samples (10 µg total protein) were reduced with dithiothreitol (DTT) (final concentration 5 mM) for 60 min at room temperature, then alkylated with iodoacetamide (final concentration 20 mM) for 60 min at room temperature. After precipitation with methanol/chloroform, the protein pellet was resuspended in 6 M urea, and then the urea concentration was reduced to < 1 M with milliQ H2O. Trypsin was added to achieve the final trypsin: protein ratio of 1:50, and the samples were digested overnight at 37°C. According to the manufacturer's instructions, peptides were purified on Waters C18 Sep-Pak cartridges. The purified peptides were dried down in a speed vac, resuspended in 2% acetonitrile/0.1% trifluoroacetic acid, and diluted 1:20 before injection. Peptides were injected into an LC-MS system comprised of a Dionex ultimate 3000 Nano LC (Liquid Chromatography) and a Thermo Q-Exactive mass spectrometer. Peptides were separated on a 50-cm-long EasySpray column (ES803; Thermo Fisher) with a 75 µm inner diameter and a 60-minute gradient of 2% to 35% acetonitrile in 0.1% formic acid and 5% dimethyl sulfoxide (DMSO) at a flow rate of 250 nl/min. The Top 15 most abundant peaks were fragmented after isolation with a mass window of 1.6 and a resolution of 17,500. The normalized collision energy was 28% (higher collisional dissociation). Raw data was imported and analyzed with Progenesis QI (Waters) using standard settings and manually refined retention time alignment. MS/MS data was searched in Mascot (Matrix Science) against a human database (fused Uniprot/Trembl, 03/2018), with oxidation (Met), deamidation (Gln/Asn) and carbamidomethylation (Cys) fixed as variable modifications. Precursor mass tolerance was set to 10 parts-per-million (ppm) and fragment tolerance to 0.04 Da. Peptide

identifications were FDR (False Discovery Rate) adjusted at 1%, and identifications with Mascot score < 20 were discarded.

Raw label-free quantitation (LFQ) data was imported and analyzed in Perseus (Max Planck Institute of Biochemistry). Differential expression was performed by conducting a two-sample independent Student t-test. Multiple testing was corrected via permutation-based FDR (False Discovery Rate) with the default software settings. Proteins were considered differentially expressed if their false discovery rate (FDR) was less than 0.05 and their fold change was greater than or equal to 1 or less than or equal to -1. G: Profiler (https://biit.cs.ut.ee/gprofiler/gost) was used for functional enrichment analysis of the differentially expressed proteins (DEPs). The enriched pathways/terms from the KEGG database and Gene ontology database, gene ontology biological process (GO: BP), gene ontology molecular function (GO: MF), and gene ontology clinical component (GO: CC) were ascertained for each set of DEPs by applying hypergeometric testing. Multiple testing was corrected by Benjamin Hochberg correction, and the significance level was set to < 0.05.The mass spectrometry proteomics data have been deposited to the ProteomeXchange Consortium via the PRIDE partner repository with the dataset identifier PXD031953.132

Bioinformatic analysis of proteomic data from placenta tissue, medium/large and small STB-EVs

Persus (Max Planck Institute of Biochemistry) was used for the analysis, along with the accompanying documentation and tutorials. To remove invalid data, we pre-processed the raw data by log transforming and filtering. Missing values were imputed at random from a normal distribution using the following parameters: width = 0.3 and downshift = 1.8. To ensure conformity to the normal distribution, the underlying distribution was visually inspected with

a histogram before and after missing data imputation. The data was then transformed further by deducting each (transformed) value from the highest occurring protein expression value.

Principal component analysis (PCA), heatmaps, and Pearson correlation matrices were used to further investigate the data. The data was analyzed using the correlation index and hierarchical clustering. A two-sample independent student t-test was used to assess differential expression. Multiple testing was corrected using permutation-based false discovery rate (FDR) with the following parameters, with significance set at less than 0.05.

Western Blotting

To further characterize and immune-phenotype, we performed western blots on placental homogenates and STB-EV pellets. The relevant primary antibodies were used to probe all STB-EVs (as discussed in the main article). An equal amount of protein (20 micrograms) was mixed with 4 X Laemmli buffer ((180 mM Tris-Cl (pH 6.8), 6% SDS, 30% glycerol, 0.3% 2-mercaptoethanol, and 0.0015% bromophenol blue, BioRad)). After heating the sample mix for ten minutes at 70^{o}C, an equal volume of the sample mix was loaded. Electrophoresis was performed at 150 V for 1.5 hours in a Novex minicell tank (Invitrogen, UK) filled with NuPAGE^{TM} MOPS SDS running buffer under reducing (for PLAP, Cytochrome C, ALIX, SR-BI, Filamin B, PAPP-A2, Collagen 17 A1) and non-reducing (for CD 63) conditions on NuPAGE TM 4-12% Bis-Tris Gel 1.0 mm x 10 well gels (Invitrogen by Thermo Fisher Scientific) (Novex by Life Technologies). As a protein size marker, Precision plus protein^{TM} dual color standards (Bio-Rad Laboratories Ltd, Hertfordshire, UK) were used. Following protein separation, the proteins were transferred to a polyvinylidene difluoride (PVDF) membrane (Bio-Rad).

In a Novex semi-dry transfer apparatus, the PVDF membrane and gel were sandwiched between four filter paper sheets pre-soaked in anode one buffer solution (300 mM Tris, 10%

methanol pH 10.4) and two filter paper sheets pre-saturated with anode two buffer solution (25 mM Tris, 20% methanol pH 10.4) at the bottom and three filter paper sheets pre-soaked in cathode buffer solution (25 mM Tris, 40 mM (Life Technologies, UK). For 45 minutes, the transfer was run at 25 V. The membranes were blocked for one hour with 5% Blotto (2BScientific) in 0.1% TBST (Tris-buffered saline (20 mM Tris, 137 mM NaCl, pH 7.6) and 1% Tween-20, Sigma), then incubated overnight with the appropriate antibody.

Antibodies used were SR-BI (ab52629 [0.35 µg/µl] 1:1000 dilution, monoclonal Rabbit, Abcam), Filamin B (GTX387 [1.64 µg/µl] 1: 1000 dilution, monoclonal mouse, Insight Biotechnology), PAPP-A2 (ab59100 [1 µg/µl] 1: 2000 dilution polyclonal Rabbit, Abcam), Collagen 17 A1(ab28440 [1 µg/µl] 1: 2000 dilution polyclonal Rabbit, Abcam), and for characterization, placental alkaline phosphatase (PLAP [1.667 µg/µl] at 1:1000 dilution in house antibody), CD 63 ([200 µg/µl]] at 1:1000 dilution, Sc-59286, Santa Cruz Biotechnology), Alix ([200µg/µl]] at 1:1000 dilution, Sc-53538, Santa Cruz Biotechnology), and Cytochrome C ([200 µg/µl]] at 1:1000 dilution, Sc-13156, Santa Cruz Biotechnology) as recommended by the international society for extracellular Vesicles (ISEV).

After an overnight incubation and three five-minute TBST washes, the membranes were incubated for an hour at room temperature with the corresponding secondary antibody, anti-mouse (P044701-2) or anti-rabbit (P044801-2) polyclonal goat immunoglobulins/ horseradish peroxidase (HRP) (1: 2000 dilution, Dako UK Ltd, Cambridgeshire UK) and rinsed three times in TBST. The membranes were developed using a gel documentation system (G-Box, Syngene, Cambridge UK) running GeneSys (version 1.5.0.0, Syngene) and a chemiluminescence film (Amersham HyperfilmTM ECL (enhanced chemiluminescence; GE Healthcare Limited, Buckinghamshire UK) to obtain the band intensity for each lane. The fold change (FC) between normal and preeclampsia samples was calculated by normalizing the comparative expression

analysis to the total protein loaded (using Amido Black stain) 17,18. The normalized densitometric values were statistically tested using a one-tailed Student t-test, with significance set at less than 0.05. Tables 1 and 2 show the reagents and antibodies used in western blot analysis, respectively. Details of western blot for STB-EV characterization and proteomic validation experiments can be seen in the supplemental material.

This study utilized 12 samples for initial discovery and 12 for targeted western blot validation

Results

Patient demographics and clinical characteristics

PE mothers (Table 1), as expected, had a significantly higher average systolic (178.83 mmHg, $P < 0.001$) and diastolic (109.17 mmHg, $P < 0.001$) blood pressure compared to normal pregnant mothers average systolic (129.50 mmHg) and diastolic (67.00 mmHg). PE women are also significantly more likely to deliver prematurely (PE = 32.00 weeks gestation NP = 39.17 weeks gestation, $P < 0.001$) and have proteinuria (PE = 2.58 pluses on urine dipstick NP = 0 pluses on urine dipstick, $P < 0.001$) compared to normal pregnancy

Finally, PE babies significantly weighed less than normal babies (PE = 1515.83g NP = 3912.50 g, $P < 0.001$). Surprisingly, we found no significant difference in body mass index, the gender of the child, and maternal age.

Table 1. General descriptive statistics of sample population

Characteristics	Sub-Classification	Normal Pregnancy	Preeclampsia	P Value
Sample size		6	6	
Maternal age years (mean (SD))		34.5 ± 5.39	36.33 ± 4.13	0.524
Systolic blood pressure mmHg (mean (SD))		129.5 ± 4.93	178.83 ± 12.56	<0.001
Diastolic blood pressure mmHg (mean (SD))		67 ± 6.2	109.17 ± 9.85	<0.001
Body mass index kg/m-2 (mean (SD))		29.92 ± 9.1	31.25 ± 11.12	0.825
Proteinuria plus(es) (mean (SD))		0	2.58 ± 1.2	<0.001
Gestational age at diagnosis in weeks (mean (SD))		NA	30.5 ± 3.50	0.001
Gestational age at delivery in weeks (mean (SD))		39.17 ± 0.98	32 ± 3.52	0.001
Birth weight grams (range)		3912.5 ± 730.4	1515.83 ± 600.57	<0.001
Intrauterine growth restriction (IUGR) = Yes (%)		0(0)	6(100)	0.004
Male new-born sex (%)		2(33.3)	2(33.3)	1.000

Characterization of syncytiotrophoblast membrane extracellular vesicles (STB-EVs)

Flow cytometry (Figure 1) was showed that many detected events (83-85 ± 8.0-8.3%) were negative for CD 235a (Red blood cells), CD41 (platelets) and HLA-I and II (white blood cells) (Figure 1B) while 92 ± 0.9% (Figure 1D and 1G) of detected events were $PLAP^{+}$ extracellular vesicles (BODIPY FL N-(2-aminoethyl)-maleimide (bioM) and placental alkaline phosphatase (PLAP) double-positive). Detergent treatment, which could break down EVs, with NP-40 confirmed that majority (99%) of our samples were largely vesicular since only 0.1 ± 0.12% of BODIPY FL N-(2-aminoethyl)-maleimide and PLAP double-positive events were detected (a reduction of 99%) (Figure 1E and 1H).

Transmission electron microscopy on 10K STB-EV pellets (Figure 2A and 2B) and 150K STB-EVs (Figure 2C and 2D) in our sample preparation showed the typical cup-shaped morphology of extracellular vesicles on transmission electron microscopy (TEM) within the appropriate size range. Western blot confirmed they express the classic syncytiotrophoblast membrane

marker, placenta alkaline phosphatase (PLAP), the extracellular vesicle markers ALIX and CD 63. In addition, they lacked the negative EV marker cytochrome C (Figure 3A). Nanoparticle tracking analysis (NTA) confirmed the homogeneity of the 150K STB-EV pellets (small STB-EVs) (Figure 3B) with a modal size of (205.8 ± 67.7) nm and the heterogeneity of the 10K STB-EV pellets (medium/large STB-EVs) (Figure 3C) with a size range of (479.4 ± 145.6) nm.

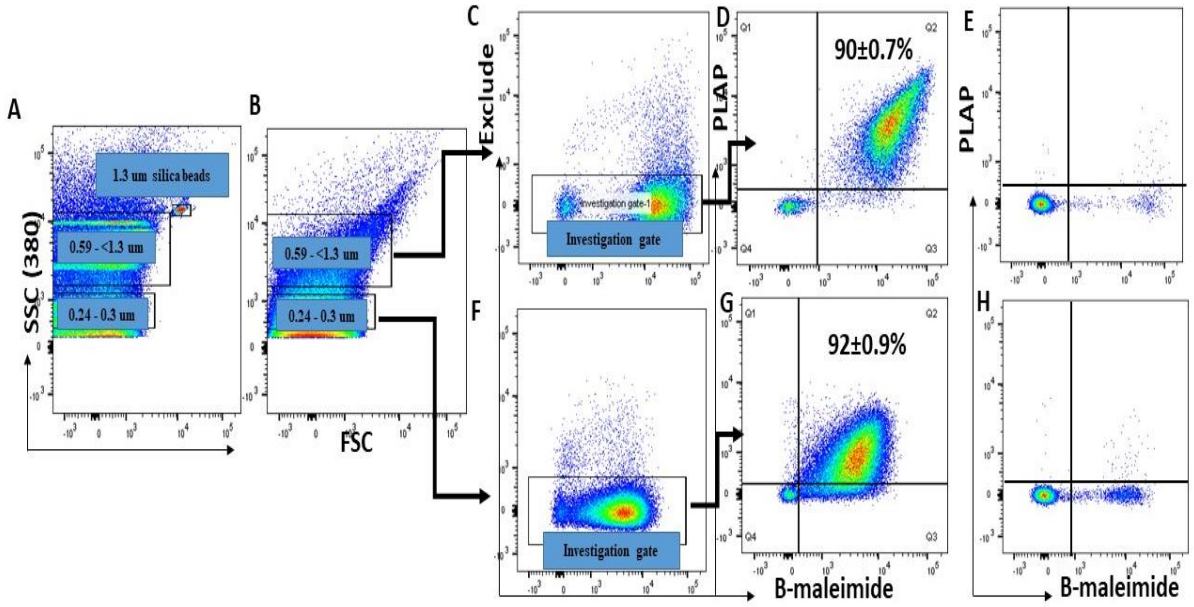

Figure 1. Flow analysis of medium/large STB-EVs in the 10K STB-EV pellet. Apogee beads mix were used to set the flow machine's light scatter resolution to 0.59-1.3 µm and 0.24-1.3 µm silica beads(A). Figure B shows the application of SSC and FSC PMTVs as determined by apogee beads mix for the analysis of m/lSTB-EVs in the 10K pellet. An investigation gate was created to include only medium/large EVs negative for non-placental markers (C & F). Extracellular vesicles from the investigation gate were further analyzed for staining by bioM and expression of PLAP (D & G). Figure E and H shows that the bioM$^+$ PLAP$^+$ EVs were

sensitive to detergent treatment. The percent of B-Maleimide^{+} PLAP^{+} from the 0.59-1.3 µm gate is consistent under both SSC conditions.

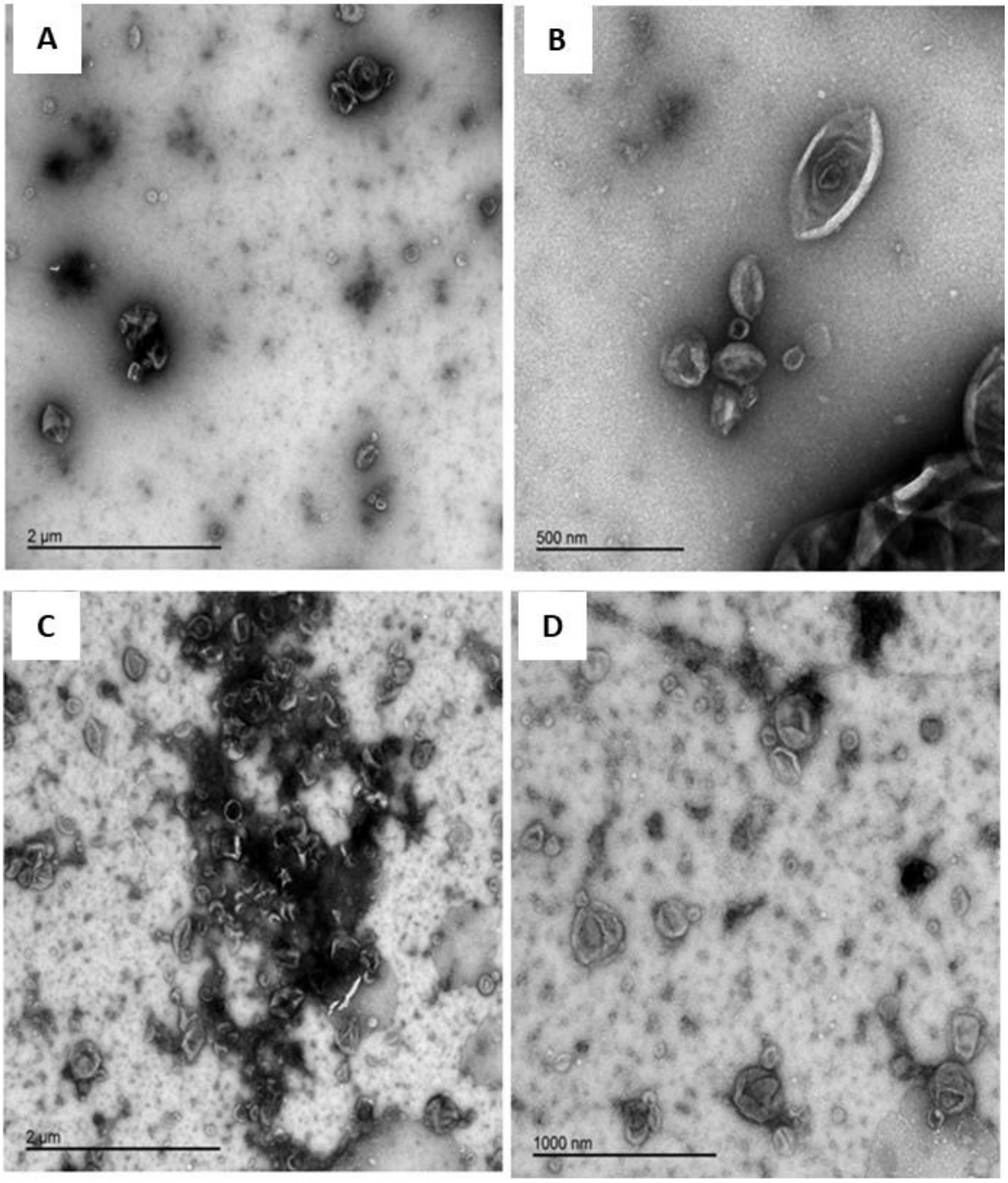

Figure 2. Results of STB-EV characterization. Figure A,B,C and D displays representative transmission electron microscopy (TEM) images with wide view (A and C), medium/large STB-EVs (B), and Small STB-EVs (D).

A

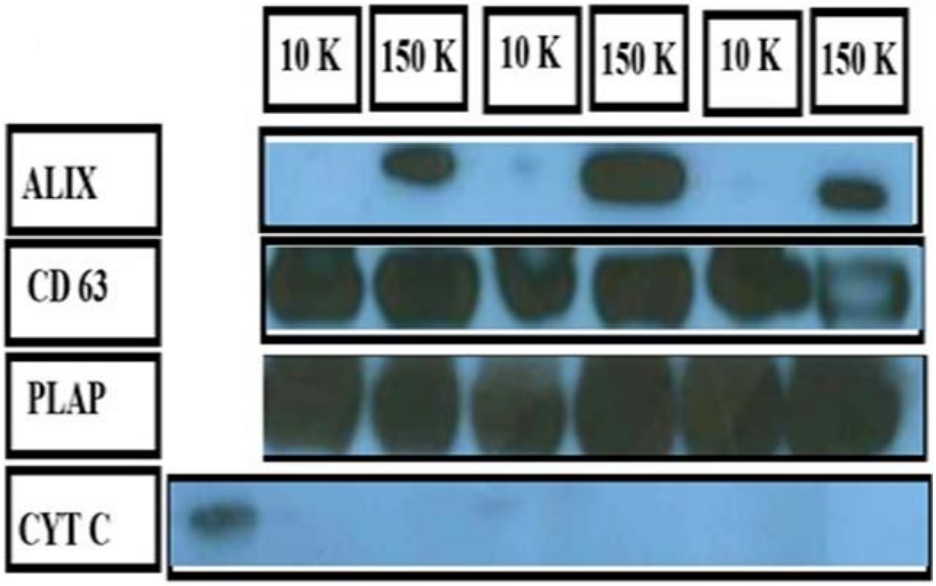

B

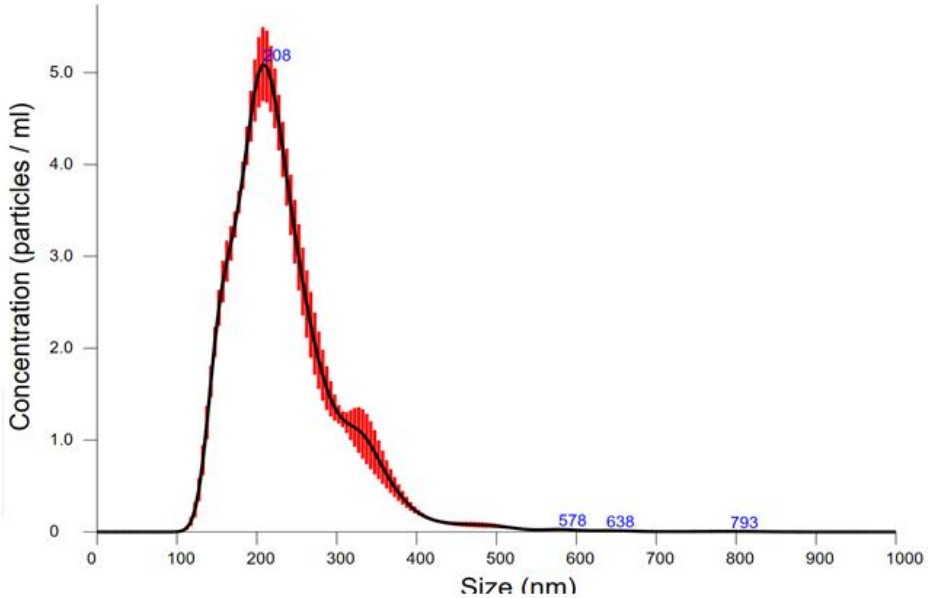

C

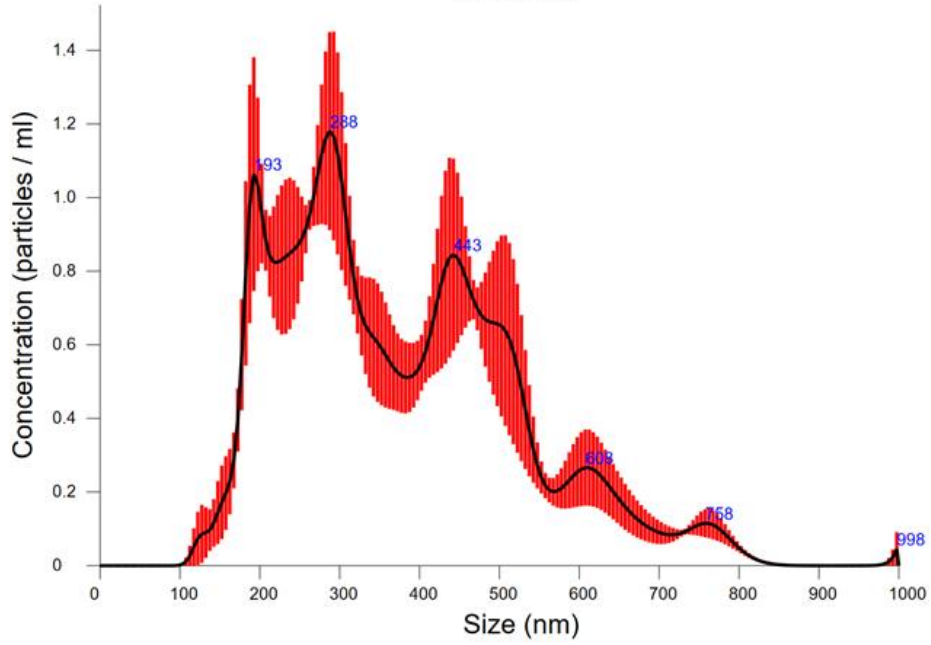

307

Figure 3. Results of STB-EV characterization. The western blot characterization of S STB-EVs and mlSTB-EVs (A). 10K refers to mlSTB-EVs and 150K refers to s STB-EVs. CYT C refers to cytochrome c. Figure 2A and 2B show the NTA results of m/lSTB-EVs (B) and sSTB-EVs (C).

Differentially carried proteins (DCPs) in Placenta homogenate, Medium/Large STB-EVs and Small STB-EVs in Preeclampsia versus normal pregnancies.

In total, using mass spectrometry, there were fifteen (15) proteins in the placenta, three hundred and four (304) in m/lSTB-EVs, and seventy-three (73) in sSTB-EVs were differentially expressed between preeclampsia (PE) and normal pregnancy (NP).

In the placenta (Table 2), *isoform HMG-R of High mobility group protein (HMGA1), Fibrinogen-like protein 1(FGL1), isoform 1 of Kinesin-like protein (KIF2A), Ig kappa chain C region (IGKC)* were the most abundant proteins based on fold change. Concomitantly, *serum paraoxonase/arylesterase 1 (PON1) and alpha-1B-glycoprotein (AIBG)* were the least abundant proteins.

For m/lSTB-EVs (Table 2), the most differentially abundant proteins were the *collagen alpha-1(XVII) chain (COL17A1), isoform 2 of Filamin-B (FLNB), tumor necrosis factor-alpha-induced protein 2 (Fragment) (TNFAIP2)* based on fold change. In contrast, the least differentially abundant proteins were *sodium-dependent phosphate transporter 1 (SLC20A1), methylthioribose-1-phosphate isomerase (Fragment) (MRI1), prostatic acid phosphatase (Fragment) (ACPP*) based on fold change.

Finally, the sSTB-EVs (Table 2) had *solute carrier family 2, facilitated glucose transporter member (SLC2A11), v-type proton ATPase 16 KDa proteolipid subunit (ATP6V0C), pappalysin 2 (PAPP-A2)* as the most differentially abundant by fold change while *sodium-*

dependent phosphate transporter 1 (SLC20A1) and *isoform 2 of ADP-ribosylation factor GTPase-activating protein (ARFGAP3)* were the least differentially abundant. There were 25 differentially carried proteins (DCPs) including *filamin B (FLNB), ERO1-like protein alpha (ERO1A), endoglin (EGLN), pappalysin-2 (PAPP-A2), siglec6 (SIGL6)* shared between m/lSTB-EVS and sSTB-EVs and only one protein, *isoform 1 of kinesin-like protein (KIF2A)* shared between the placenta and the m/l STB-EVs. Only one protein *chloride intracellular channel protein 3 (CLIC3),* was found in all three sample sub-types (Table 3)

Table 2: Top ten differentially expressed Proteins between normal and preeclampsia placentas (bold font), medium/large STB-EVs (normal font), small STB-EVs(italics)

Protein	Symbol	LFC	Adjusted P. Value
Placenta			
Isoform HMG-R of High mobility group protein HMG-I/HMG-Y	**HMGA1**	**3.14**	**0.03**
Fibrinogen-like protein 1	**FGL1**	**2.49**	**0.04**
Isoform 1 of Kinesin-like protein KIF2A	**KIF2A**	**1.47**	**0.02**
Chloride intracellular channel protein 3	**CLIC3**	**1.09**	**0.05**
Mesencephalic astrocyte-derived neurotrophic factor	**MANF**	**1.02**	**0.03**
Ig kappa chain V-I region AG	**KV101**	**-1.02**	**0.05**
Haloacid dehalogenase-like hydrolase domain-containing protein 2 (Fragment)	**K7EJQ8**	**-1.23**	**0.05**
Ig kappa chain C region	**IGKC**	**-1.27**	**0.05**
Alpha-1B-glycoprotein	**A1BG**	**-1.34**	**0.05**
Serum paraoxonase/arylesterase 1	**PON1**	**-2.18**	**<0.01**
Medium/Large STB-EVs			

Collagen alpha-1(XVII) chain	COL17A1	4.79	<0.01
Isoform 2 of Filamin B	FLNB	3.09	<0.01
Tumor necrosis factor apha-inducible protein	TNFAIP2	3.03	<0.01
Minor histocompatibility antigen	HMHA1	1.59	0.03
Bridging integrator 2	BIN2	2.33	0.02
Sodium/potassium-transporting ATPase subunit beta-1	ATP1B	1.99	0.02
ERO-1 like protein alpha	ERO1L	1.97	<0.01
Endoglin	ENG	1.82	<0.01
Methylthioribose-1-phosphate isomerase (Fragment)	MRI1	-1.96	0.04
Sodium-dependent phosphate transporter 1	S20A1/SLC17A1	-5.24	0.04
Small STB-EVs			
Solute carrier family 2, facilitated glucose transporter member 11	*SLC2A11*	*8.91*	*0.01*
V-type proton ATPase 16 kDa proteolipid subunit	*VATL*	*7.25*	*0.02*
Pappalysin-2	*PAPP2*	*3.76*	*0.02*
ERO1-like protein alpha	*ERO1A*	*3.29*	*0.02*
Isoform 2 of Creatine kinase U-type, mitochondrial	*KCRU*	*3.20*	*0.02*
SCARB1 protein	*B7ZKQ9*	*2.95*	*0.05*
Isoform 2 of Filamin-B	*FLNB*	*2.92*	*0.02*
Solute carrier organic anion transporter family member 2A1	*SO2A1*	*2.86*	*0.02*
Isoform 2 of Oligaccharyltransferase complex subunit TC	*OSTC*	*2.82*	*0.02*
SCY1-like protein 2	*SCYL2*	*2.71*	*0.02*
Sodium-dependent phosphate transporter 1	*S20A1*	*-2.93*	*0.01*

Table 3. List of overlapping differentially carried proteins in the placenta, medium/large STB-EVs and small STB-EVs

Sample types	Differentially expressed proteins (DEPs)
m/lSTB-EVs and Placenta	Kinesin-like protein
m/lSTB-EVs, sSTB-EVs and Placenta	Chloride intracellular channel protein 3
m/lSTB-EVs and sSTB-EVs	Filamin B
	Endoplasmic Reticulum Oxidoreductase Alpha
	X-linked retinitis pigmentosa GTPase regulator interacting protein 1
	Protein NDRG1
	Collagen alpha 1(XVII) chain
	Monocyte differentiation antigen CD14
	Trophoblast glycoprotein
	Heat shock-related 70 kDa protein 2
	Endoglin
	Hippocalcin-like protein 1
	SCARB1 protein
	Importin subunit alpha 7
	Protein BCAP
	Endothelial protein C receptor
	Caveolin
	Pappalysin-2
	Phosphatidylinositol 3-kinase regulatory subunit alpha
	Keratin, type I cytoskeletal 19
	Siglec6
	Protein disulfide-isomerase

	Amine oxidase [flavin-containing] A
	Copine-3
	Dolichyl-diphosphooligosaccharide
	Sodium-dependent phosphate transporter 1
	Annexin A4

352

353

354 **Validation of select proteins in the *placenta homogenate, medium/Large STB-EVs, and***
355 ***small STB-EVs***

356 We combined all the DCPs identified from the placenta, m/lSTB-EVs, and sSTB-EVs and
357 selected proteins to validate based on fold change and our placenta specificity or enrichment
358 as previously described above in the methods section. These were pappalysin A2 (*PAPP-A2),*
359 *collagen 17A1 (COL17A1), filamin B,* and *scavenger receptor class B type I (SR-BI/ SCARB1).*
360 Validation was performed by western blot on all sample sub-types.

361 In the placenta (Figure 4A and 4D), *PAPP-A2* (FC =6.39, P Value = 0.0001) and *SR-BI* (FC =
362 1.72, P Value = 0.04) were all differentially abundant in PE. *Filamin B* (FC = 2.59, P Value =
363 0.12) was differentially abundant in PE but not significant while *COL17A1* was undetectable.
364 In medium/large STB-EVs (Figure 4B and 4E), pappalysin A2 (FC =5.09, P Value = 0.004),
365 *collagen 17A1* (FC =71.21, P Value = 0.002), *filamin B* (FC =7.60, P Value = 0.014) and
366 *scavenger receptor class B type I* (FC =2.28, P Value = 0.018) were all significantly
367 differentially abundant in PE compared to normal. In sSTB-EVs (Figure 4C and 4F), only
368 *filamin B* (FC =7.73, P Value = 0.003) and *SR-BI/SCARB1* (FC =1.60, P Value = 0.002) were
369 significantly differentially abundant while *COL17A1*(FC =12.79, P Value = 0.07) and *PAPP-*
370 *A2* (FC =1.48, P Value = 0.11) were differentially abundant but not significantly so.

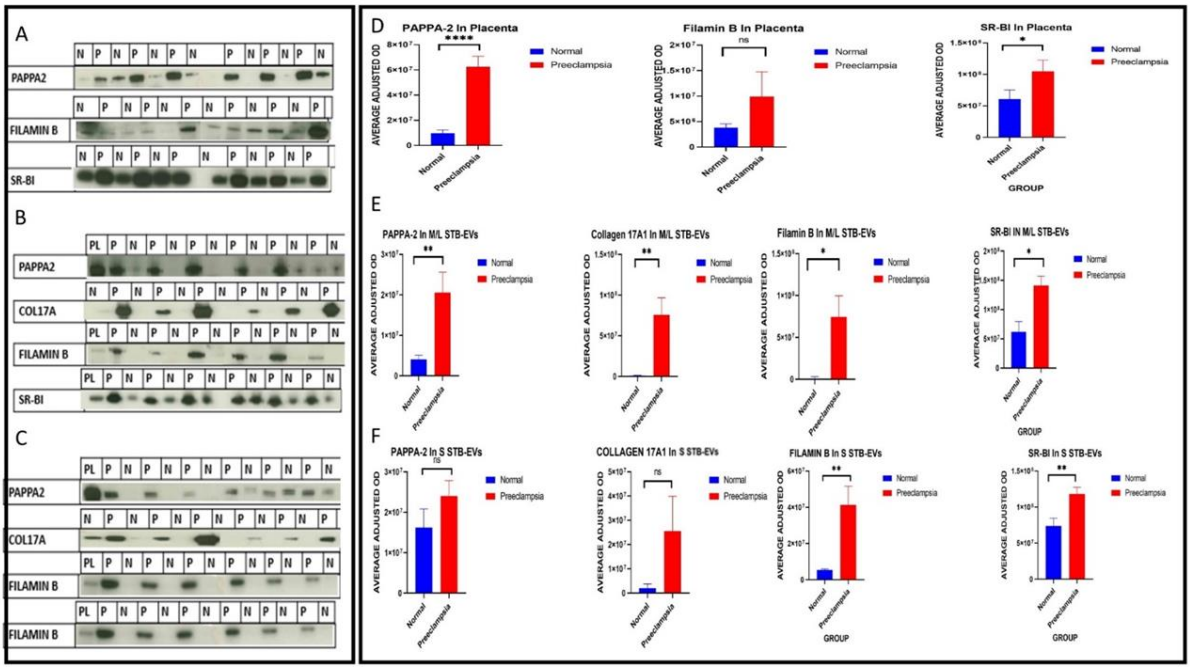

Figure 4. Figure showing the results of western blot and densitometric verification of PAPP-A2, COL17A1, FLNB and SR-BI in the placenta (A and D) m/lSTB-EVs (B and E) and sSTB-EVs (C and F). Collagen 17A1 did not show up in the placenta homogenate. * means < 0.05, ** means < 0.01, *** means < 0.001, **** means less than 0.001 and ns means non-significant.

Functional enrichment of differentially carried proteins (DCPs) in preeclampsia (PE)

We performed a functional enrichment analysis on the list of differentially carried proteins in placenta tissue, medium/large STB-EVs, and small STB-EVs to help better understand their role in preeclampsia (PE). The three sample sub-types did not have overlapping gene ontology terms or KEGG pathways. The top biological processes overrepresented in the placenta (Table 3A) were processes that involve *neurotransmitter secretion and transport*. In comparison, the enriched biological processes in the m/lSTB-EVs (supplemental table 3) *involved responses to hypoxia*. Finally, *posttranslational protein modification processes* were enriched among small STB-EVs (supplemental table 3). *Neurotrophin signaling pathway, spinocerebellar ataxia,*

and protein processing pathway were among the over enriched KEGG pathways in the placenta, m/lSTB-EVs and sSTB-EVs respectively (Supplemental table 4).

Discussion

Principal findings

In our analysis, PE and NP have different placenta and STB-EV proteomes. Four STB-EV biomarkers—filamin B, collagen 17A1, pappalysin-A2, and scavenger Receptor Class B Type 1—were verified for differential abundance. In silico investigation revealed molecular pathways such abnormal protein metabolism that may contribute to PE's clinical and pathological symptoms and inform future research.

Results in the context of what is known.

Our analysis found chloride intracellular channel 3 (CLIC3) to be the only protein differentially abundant among all sample types. CLIC3 is expressed in the placenta throughout pregnancy(Money et al., 2007) and is abundant in PE placentas compared to NP, a finding corroborated by our results. However, it has not previously been described in terms of STB-EVs. CLIC3 also recycles activated integrins back to the plasma membrane and facilitates cell migration and invasion(Dozynkiewicz et al., 2012) a process that has been identified as abnormal in PE(KHONG et al., 1986).

We found *COL17A1* to be more abundant in PE m/lSTB-EVs but not detectable in the placenta in both normal and PE. Although collagen 17 has not been described in preeclampsia, a protein of the same family, collagen 1 is deposited in higher amounts in the PE placenta and can induce preeclampsia-like symptoms by suppressing the proliferation and invasion of trophoblasts. This suppression was reversible by treating with ERK and B-catenin agonists(Feng et al., 2021). Likewise, *PAPP-A2* was significantly more abundant in the PE placenta and m/lSTB-EVs. *PAPP-A2* cleaves insulin-like growth factor binding protein (IGFBP-5 and, to a lesser

extent, IGFBP-3). PAPP-A2's mRNA and protein are differentially expressed in the placenta and maternal serum in PE patients(Whitehead et al., 2013).

Filamin B was significantly more abundant in PE m/lSTB-EVs and sSTB-EVs compared to NP. Filamin B participates in cellular structural mechanics and signal transduction by interacting with ion channels, signaling molecules, transmembrane proteins, and transcription factors(Zhou et al., 2010). It also suppresses tumor growth and metastasis(Iguchi et al., 2015). Interestingly, in contrast to our study wei et al described Filamin B as being up regulated in the placenta (Wei et al., 2019) . Wei et al used glyceraldehyde 3-phosphate dehydrogenase (GAPDH) as an internal reference while we used total protein normalization to Amido black to quantify and compare protein expression. GAPDH is an unreliable internal reference protein, particularly in preeclampsia(Lanoix et al., 2012) and this may explain these discordant findings. In addition, in our proteomics data, we found GAPDH to be among the most differentially expressed (upregulated) proteins.

Likewise, we identified scavenger receptor class B, type 1 (SCARB1/SR-BI) to be significantly increased in PE placenta, m/l and sSTB-EVs. SCARB1/SR-BI, is most abundant in the adrenal glands, placenta, liver, and brain(Ganesan et al., 2016; Shen et al., 2016). SR-BI facilitates the uptake of cholesteryl esters from high-density lipoproteins and lipid-soluble vitamin and transthyretin-bound thyroid hormone by placental trophoblast cells(Landers et al., 2018).

In terms of potential mechanisms of preeclampsia, we found no overlap in the biological processes and KEGG pathways among the three sample sub-type. In the placenta, gene ontology biological processes (GO: BP) involved in *neurotransmitter secretion and transport* were overrepresented while *platelet activation*, *MAPK* and *Rap 1 signaling* pathways were among the detected KEGG pathways. In m/lSTB-EVs, *protein modification process*, and *decreased oxygen level responses* were among the perturbed GO: BP terms. *Alzheimer's* and *prion disease* were among the identified KEGG pathways. In sSTB-EVs, *post-translational*

modification processes and *endoplasmic reticulum protein processing* were the principal GO: BP terms and KEGG pathways.

Recent research has shown that ischemic hypoxia and the release of proinflammatory cytokines in PE can cause protein misfolding and initiate endoplasmic reticulum (ER) stress due to hypoxia-reoxygenation damage to the endoplasmic reticulum(Gathiram & Moodley, 2016). PE can also cause posttranslational modifications to proteins, such as changing the isoelectric point, which results in different S-nitrosylation outcomes in placental proteins(Zhang et al., 2011). It is thought that the accumulation of these aggregates of unfolded protein response (UPR) or misfolded proteins contributes to the pathophysiology of PE(Gathiram & Moodley, 2016). Other processes and KEGG pathways have been previously described in preeclampsia, while others found in our study are new and may warrant further research(Lee et al., 2020; Wan Shumei, Peng Ping, Qiao Lin, 2019).

Ideas and Speculation

STB-EVs are liquid biomarkers with real-time information from the damaged placenta in PE due to their placenta-specificity. It would be interesting to test maternal plasma or serum samples for the four STB-EV indicators reported in our study.

It is unclear which comes first: misfolded proteins depositing in trophoblasts and preventing normal invasion, causing ischemia and endoplasmic reticulum stress, which leads to defects in trophoblast invasion, oxidative stress, and endothelial cell dysfunction, or the trophoblast invasion defects, oxidative stress, and endothelial cell dysfunction, or the misfolded proteins because of faulty invasion and oxidative stress. Further studies exploring these PE pathogenic processes would be intriguing.

462 **Strengths and limitations**

463 Our study explored the difference in the proteome between PE and NP by analyzing the
464 placenta and its extracellular vesicles. This study is one of the few to do so using extracellular
465 vesicles obtained by a physiologic technique, the *ex-vivo* dual lobe placenta perfusion.
466 However, the control population used for this study was not gestationally age-matched because
467 it is impossible to obtain the ideal control for early onset PE patients. Also, our sample size
468 was small (n of 12).

469 **Conclusion**

470 Our study may have found novel STB-EV-bound protein indicators that are significantly more
471 abundant in PE than normal. Since STB-EVs are present in the circulation from early
472 pregnancy to term and are released more in PE, these STB-EV carried proteins may help with
473 earlier diagnosis and mechanistic insights.

474 **Acknowledgments**

475 We acknowledge the support of the National Institute of Health Research Clinical Research
476 Network for assistance in patient recruitment and Fenella Roseman and Lotoyah Carty,
477 research midwives who kindly recruited the patients for this study. We acknowledge the
478 patients who kindly consented to this research study.

479 **Competing interests:**

480 The authors declare no competing interests.

481

482

483

484

References

ACOG Practice Bulletin No. 202: Gestational Hypertension and Preeclampsia. (2019). *Obstetrics and Gynecology*. https://doi.org/10.1097/AOG.0000000000003018

Awoyemi, T., Motta-Mejia, C., Zhang, W., Kouser, L., White, K., Kandzija, N., Alhamlan, F. S., Cribbs, A. P., Tannetta, D., Mazey, E., Redman, C., Kishore, U., & Vatish, M. (2021). Syncytiotrophoblast Extracellular Vesicles From Late-Onset Preeclampsia Placentae Suppress Pro-Inflammatory Immune Response in THP-1 Macrophages. *Frontiers in Immunology*, *12*. https://doi.org/10.3389/FIMMU.2021.676056

Billieux, M. H., Petignat, P., Fior, A., Mhawech, P., Blouin, J. L., Dahoun, S., & Vassilakos, P. (2004). Pre-eclampsia and peripartum cardiomyopathy in molar pregnancy: clinical implication for maternally imprinted genes. *Ultrasound in Obstetrics & Gynecology : The Official Journal of the International Society of Ultrasound in Obstetrics and Gynecology*, *23*(4), 398–401. https://doi.org/10.1002/UOG.1015

Brown, M. A., Magee, L. A., Kenny, L. C., Karumanchi, S. A., McCarthy, F. P., Saito, S., Hall, D. R., Warren, C. E., Adoyi, G., & Ishaku, S. (2018). Hypertensive disorders of pregnancy: ISSHP classification, diagnosis, and management recommendations for international practice. In *Hypertension*. https://doi.org/10.1161/HYPERTENSIONAHA.117.10803

Dozynkiewicz, M. A., Jamieson, N. B., MacPherson, I., Grindlay, J., vandenBerghe, P. V. E., vonThun, A., Morton, J. P., Gourley, C., Timpson, P., Nixon, C., McKay, C. J., Carter, R., Strachan, D., Anderson, K., Sansom, O. J., Caswell, P. T., & Norman, J. C. (2012). Rab25 and CLIC3 Collaborate to Promote Integrin Recycling from Late Endosomes/Lysosomes and Drive Cancer Progression. *Developmental Cell*, *22*(1), 131. https://doi.org/10.1016/J.DEVCEL.2011.11.008

Dragovic, R. A., Collett, G. P., Hole, P., Ferguson, D. J. P., Redman, C. W., Sargent, I. L., & Tannetta, D. S. (2015a). Isolation of syncytiotrophoblast microvesicles and exosomes and their characterisation by multicolour flow cytometry and fluorescence Nanoparticle Tracking Analysis. *Methods (San Diego, Calif.)*, *87*, 64–74. https://doi.org/10.1016/J.YMETH.2015.03.028

Dragovic, R. A., Collett, G. P., Hole, P., Ferguson, D. J. P., Redman, C. W., Sargent, I. L., & Tannetta, D. S. (2015b). Isolation of syncytiotrophoblast microvesicles and exosomes and their characterisation by multicolour flow cytometry and fluorescence Nanoparticle Tracking Analysis. *Methods*, *87*, 64–74. https://doi.org/10.1016/j.ymeth.2015.03.028

Feng, Y., Chen, X., Wang, H., Chen, X., Lan, Z., Li, P., Cao, Y., Liu, M., Lv, J., Chen, Y., Wang, Y., Sheng, C., Huang, Y., Zhong, M., Wang, Z., Yue, X., & Huang, L. (2021). Collagen I Induces Preeclampsia-Like Symptoms by Suppressing Proliferation and Invasion of Trophoblasts. *Frontiers in Endocrinology*, *12*. https://doi.org/10.3389/fendo.2021.664766

Ganesan, L. P., Mates, J. M., Cheplowitz, A. M., Avila, C. L., Zimmerer, J. M., Yao, Z., Maiseyeu, A., Rajaram, M. V. S., Robinson, J. M., & Anderson, C. L. (2016). Scavenger receptor B1, the HDL receptor, is expressed abundantly in liver sinusoidal endothelial cells. *Scientific Reports*, *6*. https://doi.org/10.1038/srep20646

Gathiram, P., & Moodley, J. (2016). Pre-eclampsia: its pathogenesis and pathophysiolgy. *Cardiovascular Journal of Africa*, *27*(2), 71–78. https://doi.org/10.5830/CVJA-2016-009

Germain, S. J., Sacks, G. P., Sooranna, S. R., Soorana, S. R., Sargent, I. L., & Redman, C. W. (2007). Systemic inflammatory priming in normal pregnancy and preeclampsia: the role of circulating syncytiotrophoblast microparticles. *Journal of Immunology (Baltimore, Md. : 1950)*, *178*(9), 5949–5956. https://doi.org/10.4049/JIMMUNOL.178.9.5949

534 Goswamia, D., Tannetta, D. S., Magee, L. A., Fuchisawa, A., Redman, C. W. G., Sargent, I.
535 L., & von Dadelszen, P. (2006). Excess syncytiotrophoblast microparticle shedding is a
536 feature of early-onset pre-eclampsia, but not normotensive intrauterine growth
537 restriction. *Placenta*, *27*(1), 56–61. https://doi.org/10.1016/J.PLACENTA.2004.11.007
538 Hailu, F. G., Yihunie, G. T., Essa, A. A., & Tsega, W. kindie. (2017). Advanced abdominal
539 pregnancy, with live fetus and severe preeclampsia, case report. *BMC Pregnancy and*
540 *Childbirth*, *17*(1). https://doi.org/10.1186/S12884-017-1437-Y
541 Iguchi, Y., Ishihara, S., Uchida, Y., Tajima, K., Mizutani, T., Kawabata, K., & Haga, H.
542 (2015). Filamin B enhances the invasiveness of cancer cells into 3D collagen matrices.
543 *Cell Structure and Function*, *40*(2). https://doi.org/10.1247/csf.15001
544 Keerthikumar, S., Gangoda, L., Liem, M., Fonseka, P., Atukorala, I., Ozcitti, C., Mechler, A.,
545 Adda, C. G., Ang, C. S., & Mathivanan, S. (2015). Proteogenomic analysis reveals
546 exosomes are more oncogenic than ectosomes. *Oncotarget*, *6*(17), 15375–15396.
547 https://doi.org/10.18632/ONCOTARGET.3801
548 KHONG, T. Y., de WOLF, F., ROBERTSON, W. B., & BROSENS, I. (1986). Inadequate
549 maternal vascular response to placentation in pregnancies complicated by pre-eclampsia
550 and by small-for-gestational age infants. *BJOG: An International Journal of Obstetrics*
551 *& Gynaecology*, *93*(10). https://doi.org/10.1111/j.1471-0528.1986.tb07830.x
552 Landers, K. A., Li, H., Mortimer, R. H., McLeod, D. S. A., d'Emden, M. C., & Richard, K.
553 (2018). Transthyretin uptake in placental cells is regulated by the high-density
554 lipoprotein receptor, scavenger receptor class B member 1. *Molecular and Cellular*
555 *Endocrinology*, *474*. https://doi.org/10.1016/j.mce.2018.02.014
556 Lanoix, D., St-Pierre, J., Lacasse, A. A., Viau, M., Lafond, J., & Vaillancourt, C. (2012).
557 Stability of reference proteins in human placenta: General protein stains are the
558 benchmark. *Placenta*, *33*(3). https://doi.org/10.1016/j.placenta.2011.12.008
559 Lee, A., Chow, L., Skeith, L., Nicholas, J. A., Poon, M.-C., Poole, A. W., & Agbani, E. O.
560 (2020). Platelet Membrane Procoagulation in Preeclampsia. *Blood*, *136*(Supplement 1).
561 https://doi.org/10.1182/blood-2020-137213
562 Lisonkova, S., & Joseph, K. S. (2013). Incidence of preeclampsia: risk factors and outcomes
563 associated with early- versus late-onset disease. *American Journal of Obstetrics and*
564 *Gynecology*, *209*(6), 544.e1-544.e12. https://doi.org/10.1016/J.AJOG.2013.08.019
565 Minciacchi, V. R., Spinelli, C., Reis-Sobreiro, M., Cavallini, L., You, S., Zandian, M., Li, X.,
566 Mishra, R., Chiarugi, P., Adam, R. M., Posadas, E. M., Viglietto, G., Freeman, M. R.,
567 Cocucci, E., Bhowmick, N. A., & Di Vizio, D. (2017). MYC Mediates Large
568 Oncosome-Induced Fibroblast Reprogramming in Prostate Cancer. *Cancer Research*,
569 *77*(9), 2306–2317. https://doi.org/10.1158/0008-5472.CAN-16-2942
570 Money, T. T., King, R. G., Wong, M. H., Stevenson, J. L., Kalionis, B., Erwich, J. J. H. M.,
571 Huisman, M. A., Timmer, A., Hiden, U., Desoye, G., & Gude, N. M. (2007). Expression
572 and Cellular Localisation of Chloride Intracellular Channel 3 in Human Placenta and
573 Fetal Membranes. *Placenta*, *28*(5–6), 429–436.
574 https://doi.org/10.1016/J.PLACENTA.2006.08.002
575 Nakahara, A., Nair, S., Ormazabal, V., Elfeky, O., Garvey, C. E., Longo, S., & Salomon, C.
576 (2020). Circulating Placental Extracellular Vesicles and Their Potential Roles During
577 Pregnancy. *Ochsner Journal*, *20*(4), 439–445. https://doi.org/10.31486/toj.20.0049
578 Raposo, G., & Stoorvogel, W. (2013). Extracellular vesicles: Exosomes, microvesicles, and
579 friends. *Journal of Cell Biology*, *200*(4), 373–383.
580 https://doi.org/10.1083/JCB.201211138
581 Raudvere, U., Kolberg, L., Kuzmin, I., Arak, T., Adler, P., Peterson, H., & Vilo, J. (2019).
582 G:Profiler: A web server for functional enrichment analysis and conversions of gene
583 lists (2019 update). *Nucleic Acids Research*, *47*(W1). https://doi.org/10.1093/nar/gkz369

584 Redman, C. (2014). Pre-eclampsia: A complex and variable disease. *Pregnancy*
585 *Hypertension*, *4*(3), 241–242. https://doi.org/10.1016/J.PREGHY.2014.04.009
586 Redman, C. W. G., Staff, A. C., & Roberts, J. M. (2022). Syncytiotrophoblast stress in
587 preeclampsia: the convergence point for multiple pathways. *American Journal of*
588 *Obstetrics and Gynecology*, *226*(2S), S907–S927.
589 https://doi.org/10.1016/J.AJOG.2020.09.047
590 Shen, W. J., Azhar, S., & Kraemer, F. B. (2016). ACTH regulation of adrenal SR-B1. In
591 *Frontiers in Endocrinology* (Vol. 7, Issue MAY).
592 https://doi.org/10.3389/fendo.2016.00042
593 Soto-Wright, V., Bernstein, M., Goldstein, D. P., & Berkowitz, R. S. (1995). The changing
594 clinical presentation of complete molar pregnancy. *Obstetrics and Gynecology*, *86*(5),
595 775–779. https://doi.org/10.1016/0029-7844(95)00268-V
596 Thadhani, R., Lemoine, E., Rana, S., Costantine, M. M., Calsavara, V. F., Boggess, K.,
597 Wylie, B. J., Simas, T. A. M., Louis, J. M., Espinoza, J., Gaw, S. L., Murtha, A.,
598 Wiegand, S., Gollin, Y., Singh, D., Silver, R. M., Durie, D. E., Panda, B., Norwitz, E.
599 R., … Kilpatrick, S. (2022). Circulating Angiogenic Factor Levels in Hypertensive
600 Disorders of Pregnancy. *NEJM Evidence*, *1*(12).
601 https://doi.org/10.1056/EVIDOA2200161
602 Tkach, M., Kowal, J., Zucchetti, A. E., Enserink, L., Jouve, M., Lankar, D., Saitakis, M.,
603 Martin-Jaular, L., & Théry, C. (2017). Qualitative differences in T-cell activation by
604 dendritic cell-derived extracellular vesicle subtypes. *The EMBO Journal*, *36*(20), 3012–
605 3028. https://doi.org/10.15252/EMBJ.201696003
606 Wan Shumei, Peng Ping, Qiao Lin, G. Y. (2019). Expression of miR-144, titin-Ab and
607 MAPK signal transduction pathway related proteins in pre-eclampsia patients.
608 *INTERNATIONAL JOURNAL OF CLINICAL AND EXPERIMENTAL MEDICINE*,
609 *11*(127), 11–20. www.ijcem.com /ISSN:1940-5901/IJCEM0098123
610 Wei, J., Fu, Y., Mao, X., Jing, Y., Guo, J., & Ye, Y. (2019). Decreased Filamin b expression
611 regulates trophoblastic cells invasion through ERK/MMP-9 pathway in pre-eclampsia.
612 *Ginekologia Polska*, *90*(1), 39–45. https://doi.org/10.5603/GP.2019.0006
613 Whitehead, C. L., Walker, S. P., Ye, L., Mendis, S., Kaitu'u-Lino, T. J., Lappas, M., & Tong,
614 S. (2013). Placental specific mRNA in the maternal circulation are globally dysregulated
615 in pregnancies complicated by fetal growth restriction. *Journal of Clinical*
616 *Endocrinology and Metabolism*, *98*(3). https://doi.org/10.1210/jc.2012-2468
617 Zabel, R. R., Bär, C., Ji, J., Schultz, R., Hammer, M., Groten, T., Schleussner, E., Morales-
618 Prieto, D. M., Markert, U. R., & Favaro, R. R. (2021). Enrichment and characterization
619 of extracellular vesicles from ex vivo one-sided human placenta perfusion. *American*
620 *Journal of Reproductive Immunology (New York, N.Y. : 1989)*, *86*(2).
621 https://doi.org/10.1111/AJI.13377
622 Zeisler, H., Llurba, E., Chantraine, F., Vatish, M., Staff, A. C., Sennström, M., Olovsson, M.,
623 Brennecke, S. P., Stepan, H., Allegranza, D., Dilba, P., Schoedl, M., Hund, M., &
624 Verlohren, S. (2016). Predictive Value of the sFlt-1:PlGF Ratio in Women with
625 Suspected Preeclampsia. *The New England Journal of Medicine*, *374*(1), 13–22.
626 https://doi.org/10.1056/NEJMOA1414838
627 Zhang, H. H., Wang, Y. P., & Chen, D. B. (2011). Analysis of nitroso-proteomes in
628 normotensive and severe preeclamptic human placentas. *Biology of Reproduction*, *84*(5),
629 966–975. https://doi.org/10.1095/BIOLREPROD.110.090688
630 Zhou, A. X., Hartwig, J. H., & Akyürek, L. M. (2010). Filamins in cell signaling,
631 transcription and organ development. In *Trends in Cell Biology* (Vol. 20, Issue 2).
632 https://doi.org/10.1016/j.tcb.2009.12.001
633

Supplemental Material

Supplemental Methods

Supplemental table S1-4

Supplemental figure S1

List of differentially abundant proteins and functional enrichment analysis:

https://data.mendeley.com/datasets/j2x4h9ddcj/draft?a=8ccd383c-c6e5-495d-b66b-29c691608995

675

676

677

678

679

680

681

682

683

684 **Supplemental data**

685

686

687

688

689

690

691

692

Supplemental methods

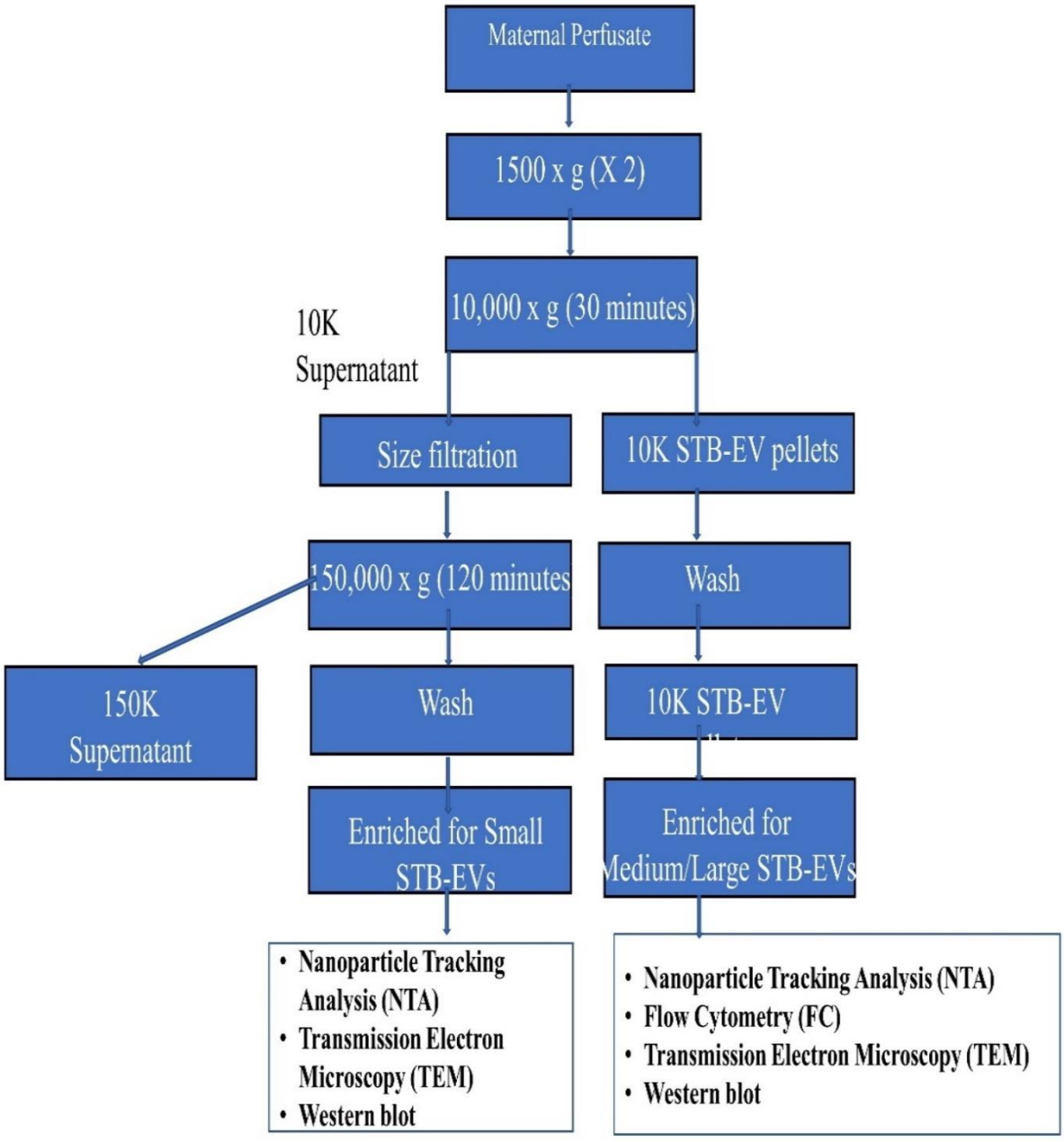

Supplemental figure 1. Flow chart illustrating the steps involved in characterizing m/lSTB-EVs and sSTB-EVs obtained via differential ultracentrifugation (10,000 and 150,000 g) of maternal perfusate. Nanoparticle trafficking analysis, transmission electron microscopy, flow cytometry, and western blot were used to characterize the pellets from both spins.

700 **Transmission electron microscopy**

701 The Sir William Dunn School of Pathology was contracted to perform transmission electron
702 microscopy. STB-EV pellets were diluted with fPBS to produce STB-EV solutions with
703 concentrations ranging from 0.1 to 0.3 g/l. For 2 minutes, ten microliter of the STB-EV pellet
704 solution was applied to freshly glowing discharged carbon formvar 300 mesh copper grids,
705 blotted with filter paper, stained with 2% uranyl acetate for 10 seconds, blotted, and air-dried.
706 The grid's STB-EV pellets are negatively stained to increase the contrast between the STB-EV
707 pellets and the background. The grids were imaged with a Gatan OneView CMOS camera on
708 an FEI Tecnai 12 TEM at 120 kV.

709 **Nanoparticle tracking analysis.**

710 The Nanosight NS500 (instrument equipped with a 405 nm laser [Malvern UK]), sCMOS
711 camera, and nanoparticle tracking analysis (NTA) software version 2.3, Build 0033 (Malvern
712 UK)) system wased used for the analysis. Instrument performance was tested with silica 100
713 nm microspheres prior to sample analysis (Polysciences, Inc.). The samples were diluted in
714 fPBS to a concentration to 1/100,000 based on the starting concentration. The samples were
715 automatically injected into the sample chamber with a 1 ml syringe using the EV measurement
716 script: prime, delay of 5, capture of 60, and repeat of 4. Camera images of the analyzed samples
717 were captured at a level of 12. (Camera shutter speed; 15 ms and Camera gain; 350). NTA
718 post-acquisition settings were optimized and maintained constant across samples. Each video
719 recording was analyzed to determine the size and concentration profile of STB-EV.

720

721

Western blotting

Supplemental table 1. Reagents used for western blot.

Buffers	Power of hydrogen (pH)	Constituents
4X Laemmli reducing buffer	6.8	9 parts 4 X Laemmli buffer
		1 part 2-beta-mercaptoethanol
4X Laemmli non-reducing buffer		4 X Laemmli buffer
Anode buffer 1	10.4	300 mM Tris base (36.34 g/L)
		100 % methanol (20 mL/L)
		980 ml of ddH_2O
Anode buffer 2	10.4	25 mM Tris base (3.0 g/L)
		100 % methanol (20 mL/L)
		980 ml of ddH_2O
Cathode buffer	9.4	25 mM Tris base (3.0 g/L)
		40 nM 6-aminocaproic acid (5.2 g/L)
		100 % methanol (20 mL/L)
		980 mL of dH2o
10 X TBS	8	NaCl (87.6g)
		Tris base (12.1g)
		700 ml of ddH_2O
TBST	8	10 X TBS (100 mL)
		0.1 % Tween-20 (1 mL)
		900 mL of ddH_2O
5% Milk TBST		5g of Blotto in 100 mL of TBST

Supplemental table 2. Antibodies used for western blot.

Antibodies	Concentration	Dilution	Antigen	Specificity	Manufacturer
Anti-PLAP (NDOG 2)	1.6 µg/µl	1/1000	PLAP	STB-EV	In house antibody
Anti-CD63	200 µg/µl	1/1000	CD63	STB-EV	Santa Cruz Biotechnology
Anti-ALIX	200 µg/µl	1/1000	ALIX	S STB-EV	Cell Signalling
Anti-Cytochrome C	200 µg/µl	1/500	Cytochrome C	Placenta homogenate	Santa Cruz Biotechnology
Anti-SR-BI	0.35 µg/µl	1/1000	SR-BI	N/A	Abcam
Anti-Filamin B	1.64 µg/µl	1/1000	Filamin B	N/A	Insight Biotechnology
Anti-PAPP-A2	1 µg/µl	1/2000	PAPP-A2	N/A	Abcam
Anti-Collagen 17 A1	1 µg/µl	1/1000	Collagen 17 A1	N/A	Abcam
Polyclonal goat-anti-mouse/rabbit immunoglobulin HRP		1/2000	Mouse and Rabbit Immunoglobulins	N/A	Dako UK Ltd

Bioinformatic analysis of proteomic data from placenta tissue, medium/large and small STB-EVs

Persus (Max Planck Institute of Biochemistry) was used for the analysis, along with the accompanying documentation and tutorials. To remove invalid data, we pre-processed the raw data by log transforming and filtering. Missing values were imputed at random from a normal distribution using the following parameters: width = 0.3 and downshift = 1.8. To ensure conformity to the normal distribution, the underlying distribution was visually inspected with a histogram before and after missing data imputation. The data was then transformed further by deducting each (transformed) value from the highest occurring protein expression value.

Principal component analysis (PCA), heatmaps, and Pearson correlation matrices were used to further investigate the data. The data was analyzed using the correlation index and hierarchical clustering. A two-sample independent student t-test was used to assess differential expression. Multiple testing was corrected using permutation-based false discovery rate (FDR) with the following parameters, with significance set at less than 0.05.

747 ***Functional enrichment of differentially expressed proteins (DEPs) in preeclampsia (PE)***

748 **Supplemental table 3**: The top three functionally enriched gene ontologies are: biological
749 process (GO: BP) Placenta (bold font), medium/large STB-EVs (normal font), and small STB-
750 EVs (italics).

751

Biological Process (BP)	Adjusted P Values	No of Proteins in BP terms	No of DEP queried	No of DEP found in BP terms
Negative regulation of neurotransmitter secretion	**0.02**	**2**	**14**	**2**
Negative regulation of synaptic vesicle exocytosis	**0.02**	**2**	**14**	**2**
Negative regulation of neurotransmitter transport	**0.05**	**3**	**14**	**2**
Response to decreased oxygen levels	0.00	84	293	30
Cellular response to decreased oxygen levels	0.00	59	293	24
Cellular ketone metabolic process	0.00	65	293	26
Peptidyl-asparagine modification	*0.02*	*10*	*73*	*5*
Protein N-linked glycosylation via asparagine	*0.02*	*10*	*73*	*5*
Protein N-linked glycosylation	*0.02*	*16*	*73*	*6*

752

753

754

755

756

757

758

759

760

761

762 **Supplemental table 4**: The top three functionally enriched KEGG Pathways in the placenta,
763 medium/large STB-EVs, and small STB-EVs (only 1 KEGG). Placenta (bold font),
764 medium/large STB-EVs (normal font), and small STB-EVs (italics)

KEGG Pathways (KP)	Adjusted P Values	No of Proteins in KP terms	No of DEP queried	No of DEP found in KP terms
Neurotrophin signalling pathway	**0.00**	**13**	**14**	**3**
Long-term potentiation	**0.01**	**6**	**14**	**2**
Renal cell carcinoma	**0.02**	**11**	**14**	**2**
Proteasome	0.00	35	293	17
Spinocerebellar ataxia	0.00	48	293	21
Alzheimer disease	0.01	94	293	29
Protein processing in endoplasmic reticulum	*0.02*	*60*	*73*	*10*

765
766 **Major Resources Table**

767 **Antibodies**

Target antigen	Vendor or Source	Catalog #	Working concentration	Dilution
PLAP	In house antibody		1.6 µg/µl	1/1000
CD63	Santa Cruz Biotechnology	sc-365604	200 µg/µl	1/1000
ALIX	Cell Signalling	#2171	200 µg/µl	1/1000
Cytochrome C	Santa Cruz Biotechnology	sc-13560	200 µg/µl	1/500
SR-BI	Santa Cruz Biotechnology	ab52629	0.35 µg/µl	1/1000
Filamin B	Insight Biotechnology	GTX387	1.64 µg/µl	1/1000
PAPP-A2	Abcam	ab59100	1 µg/µl	1/1000
Collagen 17A1	Abcam	Ab28440	1 µg/µl	1/2000
Mouse Immunoglobulins	Dako UK Ltd	P044701	1 µg/µl	1/2000
Rabbit Immunoglobulins	Dako UK Ltd	P044801	1 µg/µl	1/2000

768
769
770
771
772
773
774
775
776
777
778
779
780
781

782 **Flow cytometry resources**

Markers	Fluorochromes	Clone	CAT	Isotype	Dilution / Concentration
CD41	PE Vio770	REA386	130-105-562	REA	1 in 50 for dump channel analysis.
CD235	PE Vio770	RAE-175	130-100-258	REA	
HLA Class-I (ABC)	PE Vio770	REA230	130-101-460	REA	
HLA Class-II (DRDPDQ)	PE Vio770	RAE-332	130-104-828	REA	
REA control				REA	
CD41	Pacific blue	HIP8	303713	Mouse IgG1	1 in 100
CD235	Pacific blue	HI264	349107	Mouse IgG2a	1 in 100
HLA Class-I (ABC)	Pacific blue	W6/32	311417	Mouse IgG2a	1 in 100
PLAP	PE	Mouse mAb	N/A	IgG1	0.2mg/ml
IgG2a isotype control	Pacific blue	MOPC-173	981904	IgG2a	1 in 500
IgG1 isotype control	Pacific blue	MOPC-21	400131	IgG1	1 in 200
bioM	FITC	NA	NA	NA	0.5-1nM

783
784
785
786
787
788
789